Electronic Supplementary Material (ESI) for Journal of Materials Chemistry A.

Supporting Information of

Tungsten dichalcogenide $WS_{2x}Se_{2-2x}$ films *via* single source precursor low-pressure CVD and their (thermo-)electric properties

V. Sethi,[a] D. Runacres,[b] V. Greenacre,[b] L. Shao,[b] A. L. Hector,[b] W. Levason,[b] C. H. de Groot,[a] G. Reid[b*] and R. Huang[a*]

[a]School of Electronics and Computer Science, University of Southampton, Southampton, SO17 1BJ, UK.
[b]School of Chemistry, University of Southampton, Southampton, SO17 1BJ, UK.

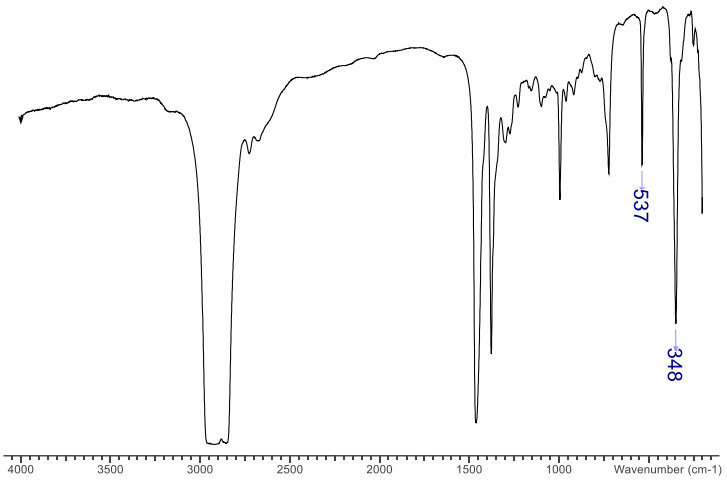

Figure S1: IR spectrum of $[WSCl_4(S^nBu_2)]$ (**1**) (Nujol / cm^{-1})

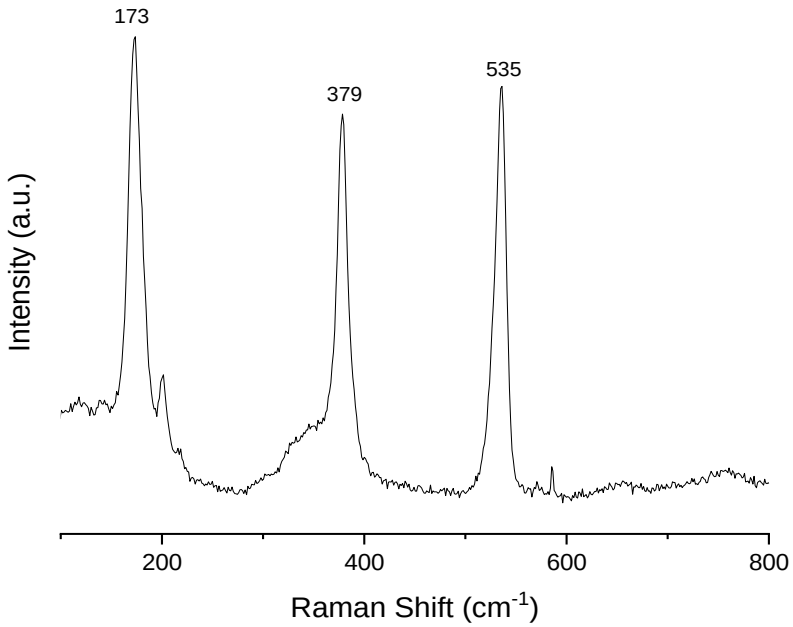

Figure S2: Raman spectrum for $[WSCl_4(S^nBu_2)]$ (**1**) (cm^{-1}).

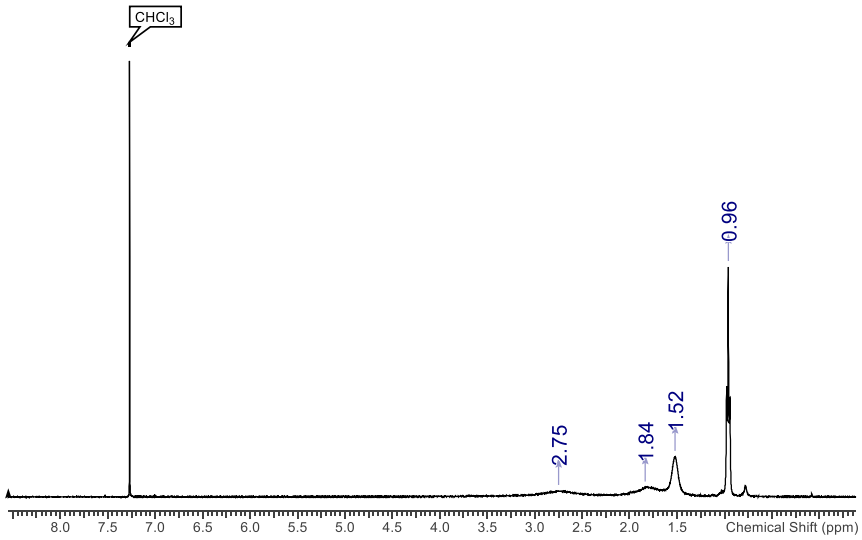

Figure S3: ^{1}H NMR spectrum of [$WSCl_4(S^nBu_2)$] (**1**) in $CDCl_3$.

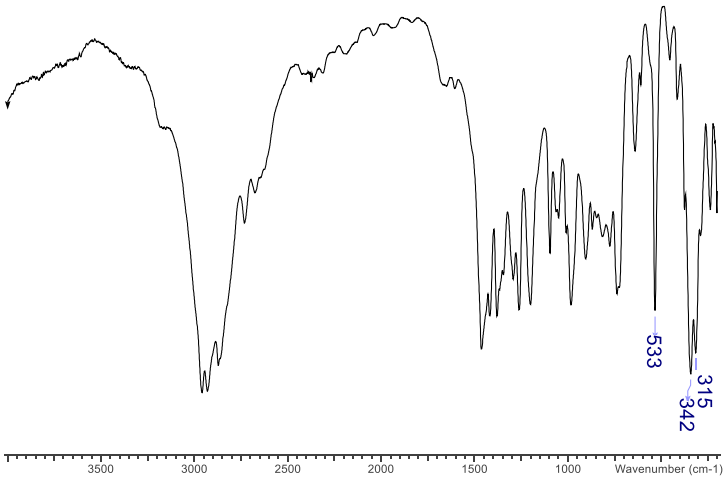

Figure S4: IR spectrum of [$WSCl_4(Se^nBu_2)$] (**2**) (Nujol / cm^{-1}).

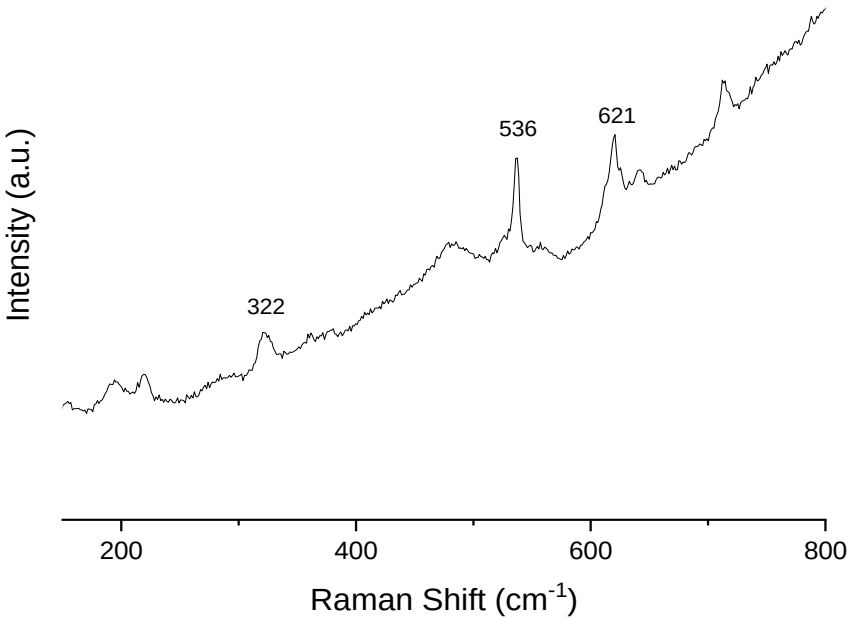

Figure S5: Raman spectrum for $[WSCl_4(Se^nBu_2)]$ (**2**) (cm^{-1}).

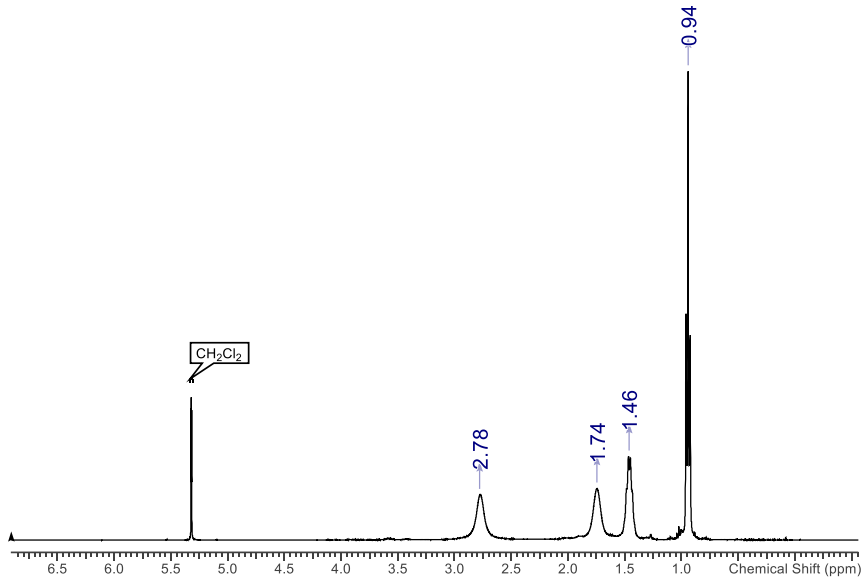

Figure S6: ^1H NMR spectrum of $[WSCl_4(Se^nBu_2)]$ (**2**) in CD_2Cl_2.

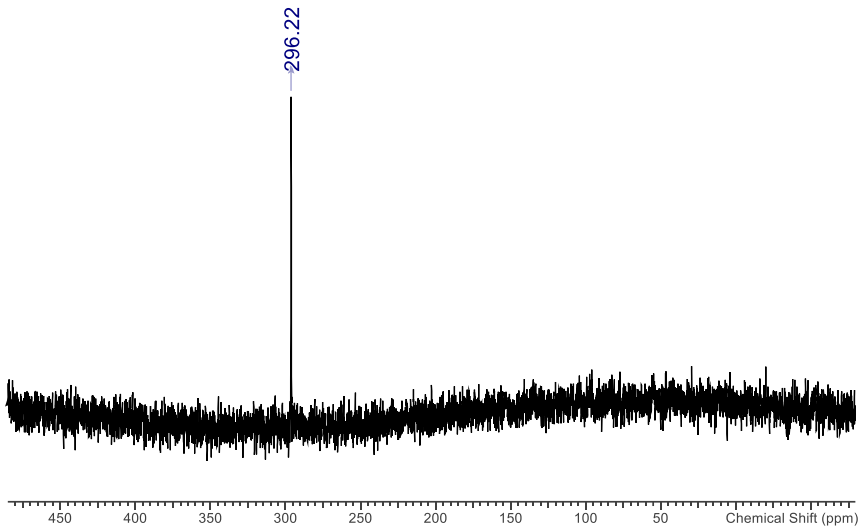

Figure S7: $^{77}Se\{^{1}H\}$ NMR spectrum of $[WSCl_4(Se^nBu_2)]$ (**2**) in CD_2Cl_2.

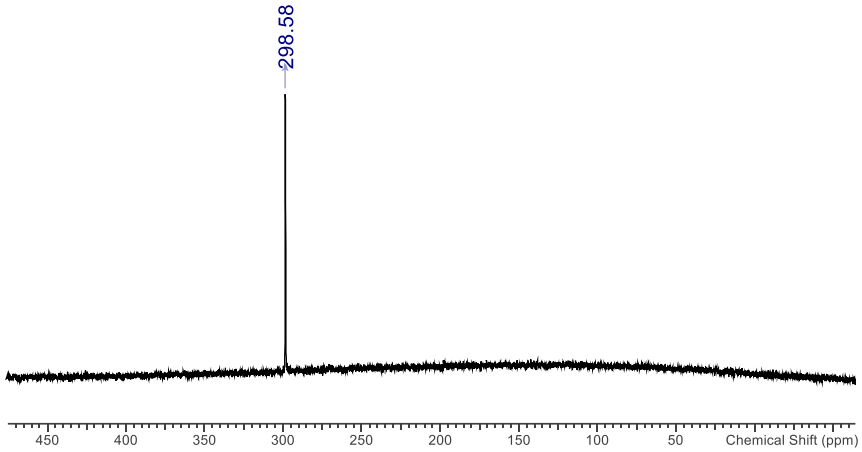

Figure S8: $^{77}Se\{^{1}H\}$ NMR spectrum of $[WSCl_4(Se^nBu_2)]$ (**2**) in CD_2Cl_2 at –90 °C.

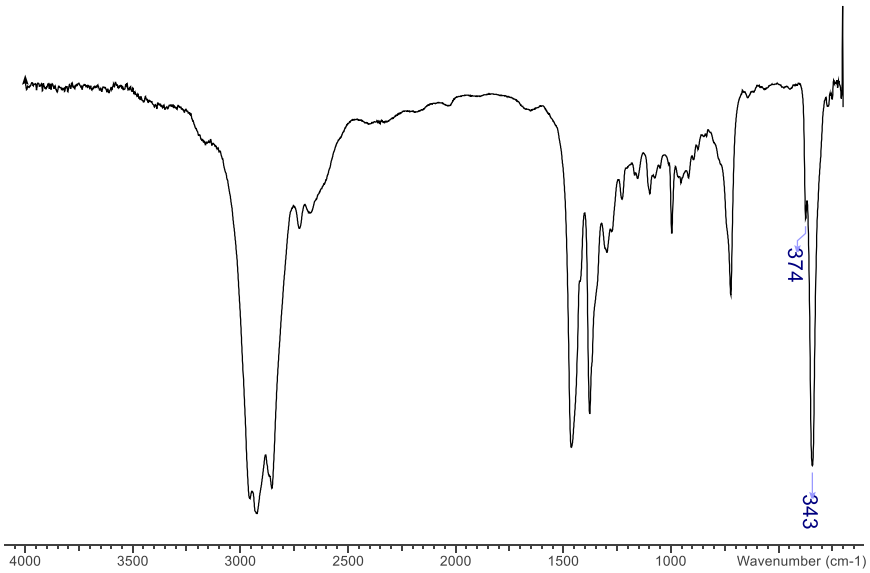

Figure S9: IR spectrum of $[WSeCl_4(S^nBu_2)]$ (**3**) (CH_2Cl_2 solution in Nujol / cm^{-1}).

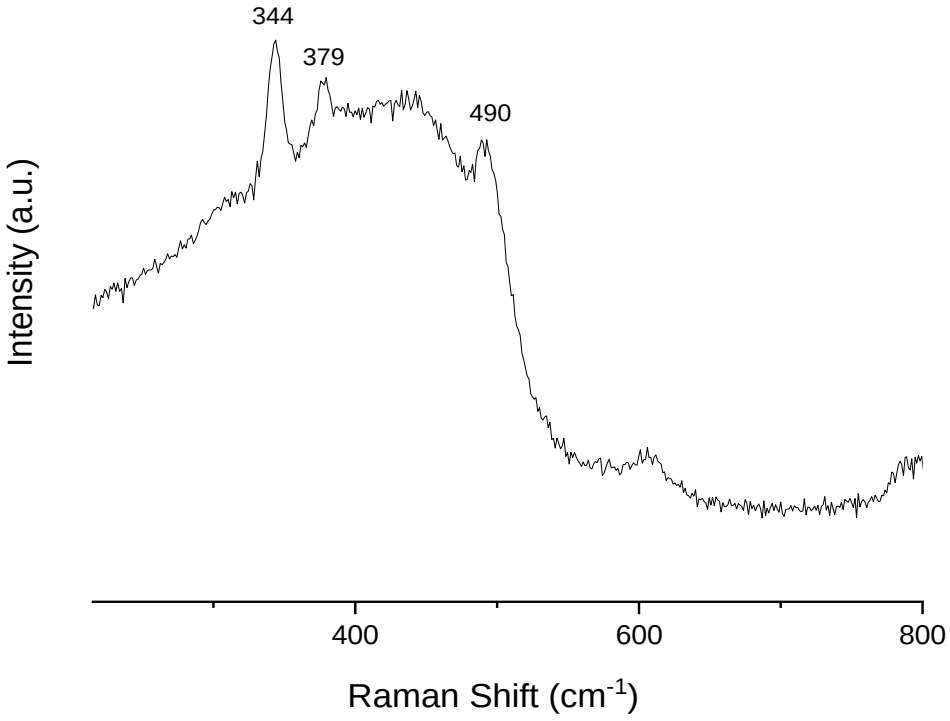

Figure S10: Raman spectrum for [$WSeCl_4(S^nBu_2)$] (**3**) (cm^{-1}).

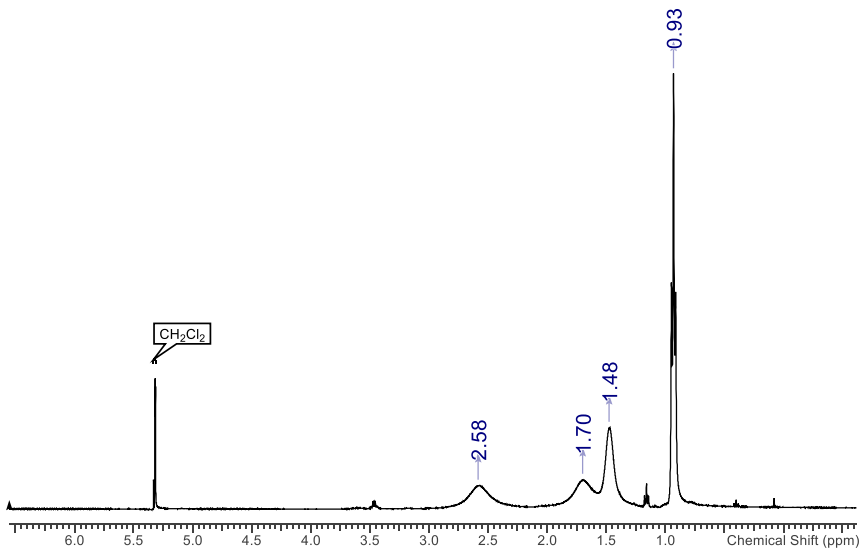

Figure S11: ^1H NMR spectrum of [$WSeCl_4(S^nBu_2)$] (**3**) in CD_2Cl_2.

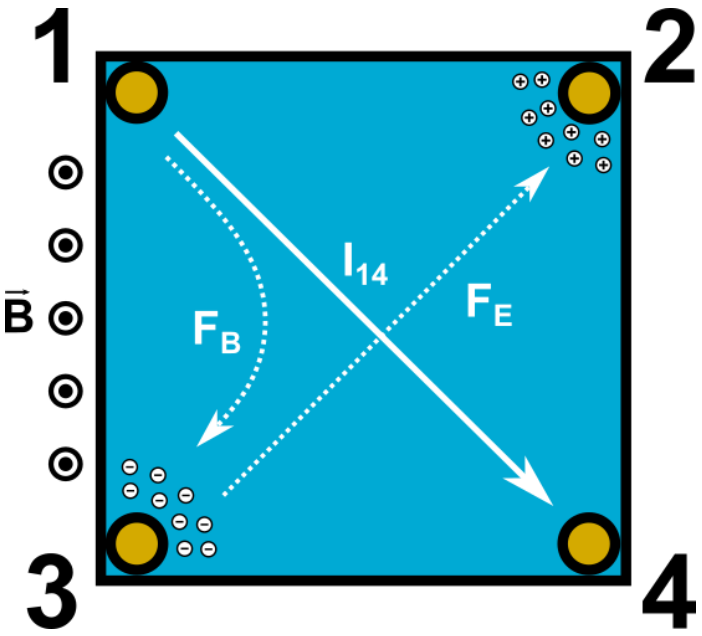

Figure S12: Visual depiction of a typical Hall measurement, with a current applied between contact 1 and 4 (I_{14}). A magnetic field ($\vec{B}$ = 0.5T) is applied orthogonal to the sensing plane, with the visual depiction showing the case for a magnetic field out of the page. The Lorentz force (F_B) defects charge carrier to one side of the sample which subsequently induces a electric field which exerts a force (F_E)which induces a Hall voltage which is measured between contacts 2 and 3. This is repeated in four contact configurations, (i.e. I_{14} , I_{41}, I_{23}, I_{32}).

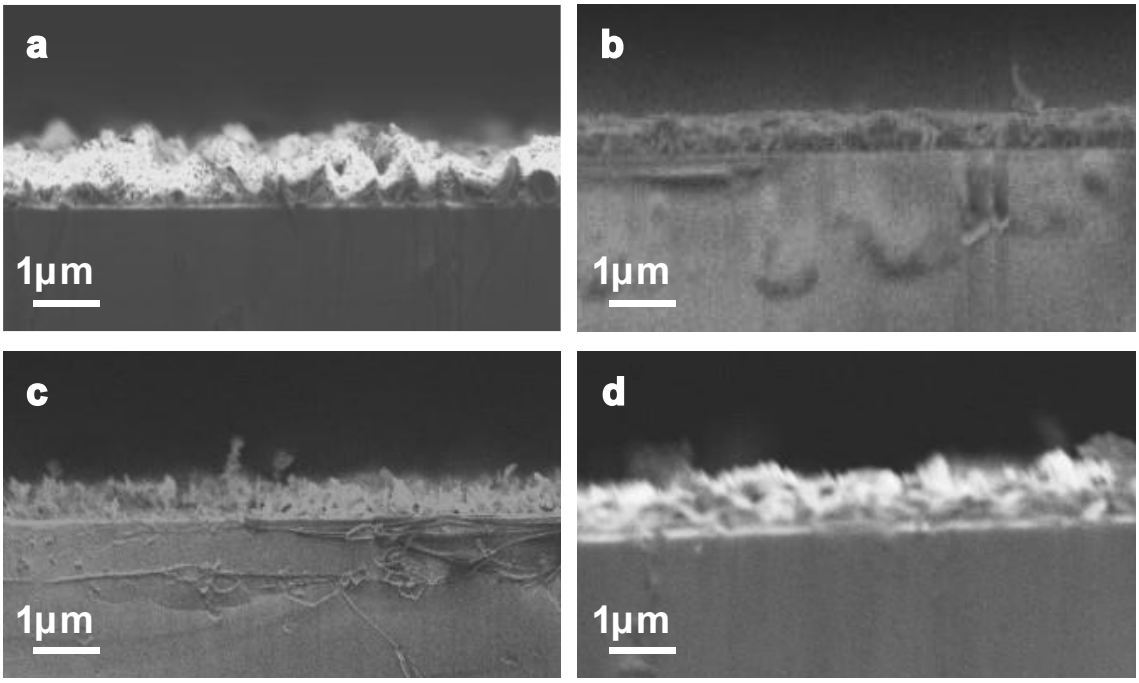

Figure S13: Cross-sectional SEM images of $WS_{2x}Se_{2-2x}$ films produced *via* low-pressure CVD, where a-d represents films produced from SSPs (**1**)-(**4**), respectively.

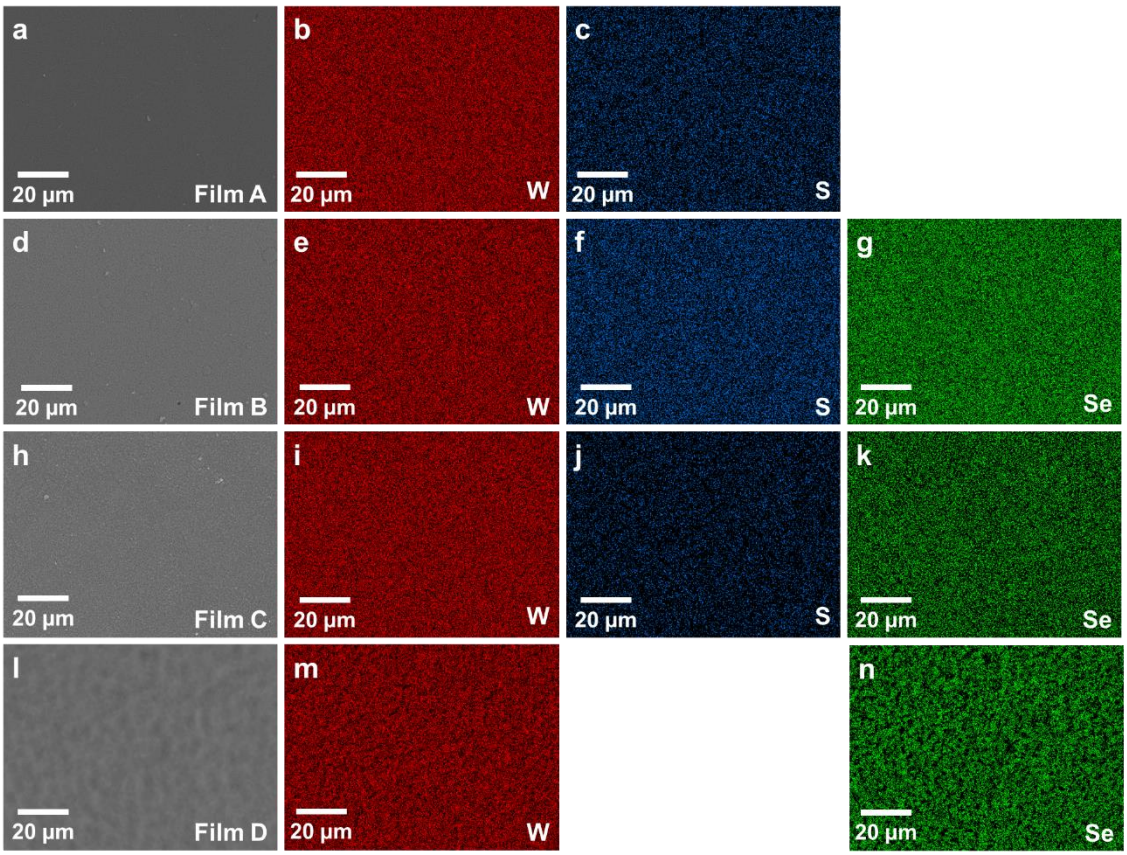

Figure S14: SEM image and associated EDX element mapping of film **A** (a-c); film **B** (d-g); film **C** (h-k); and film **D** (l-n).

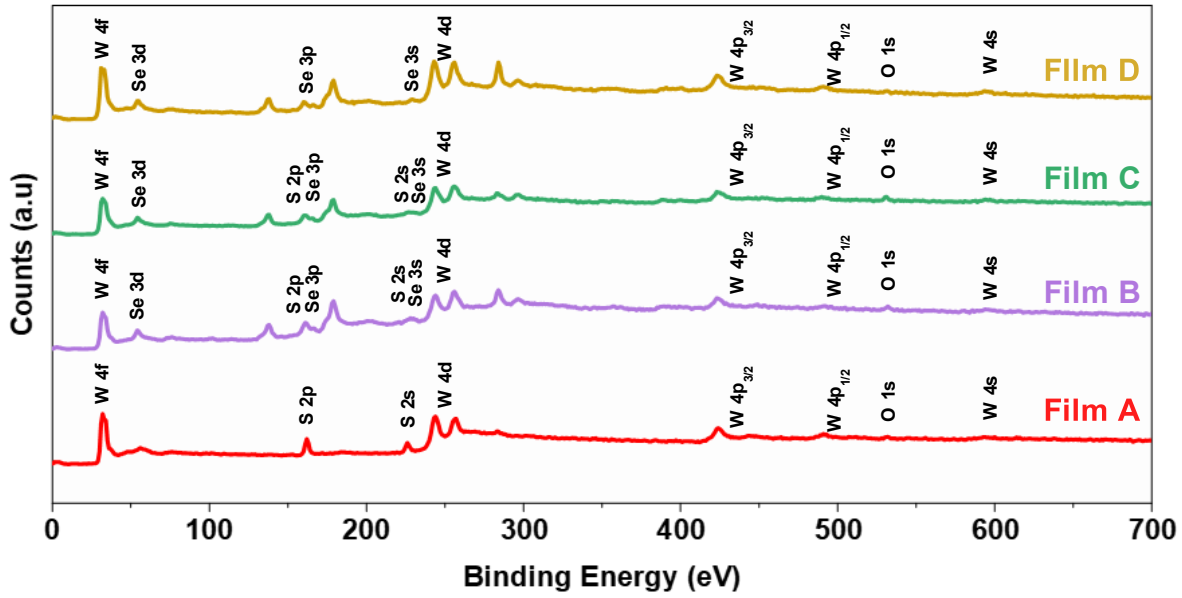

Figure S15: Survey scans over the range 0 -700 eV for all as-deposited $WS_{2x}Se_{2-2x}$ films deposited from precursors (**1**)-(**4**), with the atomic orbitals labelled. The remaining peaks are related to Auger electron detection.